# Stochastic bifurcations in a bistable Duffing–Van der Pol oscillator with colored noise

Yong Xu,[1,*] Rencai Gu,[1] Huiqing Zhang,[1] Wei Xu,[1] and Jinqiao Duan[2]

[1]*Department of Applied Mathematics, Northwestern Polytechnical University, Xi'an 710072, China*

[2]*Department of Applied Mathematics, Illinois Institute of Technology, Chicago, Illinois 60616, USA*

(Received 14 December 2010; revised manuscript received 16 April 2011; published 26 May 2011)

This paper aims to investigate Gaussian colored-noise-induced stochastic bifurcations and the dynamical influence of correlation time and noise intensity in a bistable Duffing–Van der Pol oscillator. By using the stochastic averaging method, theoretically, one can obtain the stationary probability density function of amplitude for the Duffing–Van der Pol oscillator and can reveal interesting dynamics under the influence of Gaussian colored noise. Stochastic bifurcations are discussed through a qualitative change of the stationary probability distribution, which indicates that system parameters, noise intensity, and noise correlation time, respectively, can be treated as bifurcation parameters. They also imply that the effects of multiplicative noise are rather different from that of additive noise. The results of direct numerical simulation verify the effectiveness of the theoretical analysis. Moreover, the largest Lyapunov exponent calculations indicate that *P* and *D* bifurcations have no direct connection.

DOI: 10.1103/PhysRevE.83.056215 PACS number(s): 82.40.Bj, 02.30.Oz, 02.50.−r, 05.10.Gg

## I. INTRODUCTION

Various physical, chemical, and biological processes can be modeled as nonlinear dynamical systems in which oscillatory motions are influenced by internal or external noise [1–3]. The investigation of the influence of random forces on dynamical behaviors, especially bifurcation phenomena, is one of the intensively developing research subjects [4–14]. However, the theory of stochastic bifurcations is still in its infancy [15]. There are few rigorous general theorems and criteria to detect stochastic bifurcations, which are often only verified by computer simulations or for some particular models. In fact, it is much harder to deal with stochastic bifurcation problems than deterministic bifurcation problems. The definition of deterministic bifurcation is based on the sudden change of topological properties of the phase portraits, while stochastic bifurcations may be characterized with a qualitative change of the stationary probability distribution, e.g., a transition from unimodal to bimodal distribution. At present, there are mainly two definitions for stochastic bifurcations. One is based on the sudden change of shape of the stationary probability density function—the so-called phenomenological (*P*) bifurcation; and the other is based on the sudden change of sign of the largest Lyapunov exponent—the so-called dynamical (*D*) bifurcation [15]. *D* bifurcation is a dynamical concept, which is similar in nature to deterministic bifurcations, while *P* bifurcation is a static concept. Unfortunately, these two definitions do not agree well, and this means that a new definition of stochastic bifurcation may be explored.

As we know, random noise may induce a shift of the bifurcations with respect to different control parameter values compared to their deterministic counterparts. New types of dynamics can be found in the presence of random excitations, generally referred to as the noise-induced effects. The Gaussian white noise in most theoretical studies is employed as the random driving force due to its mathematical simplicity, while realistic models of physical systems require considering colored noise. There has been a growing interest in the theoretical study of nonlinear dynamical systems subject to colored noise with a finite correlation time scale [16,17]. It has been realized that colored noise gives rise to new intriguing effects such as the reentrant phenomenon in a noise-induced transition [18] and a resonant activation in bistable systems [19].

The Duffing–Van der Pol oscillator is a prototypical system in modeling certain physical phenomena, and its simple nonlinear structure has given rise to thorough studies of its dynamical behaviors [20,21]. The Gaussian white noise was reported to create a purely noise-induced *D* bifurcation with a single attractor in the Duffing–Van der Pol system [12]. Stochastic bifurcation recently has been discussed for a self-sustained bistable Duffing–Van der Pol oscillator subject to additive Gaussian white noise in Ref. [13]. It is desirable to understand stochastic bifurcations in the bistable Duffing–Van der Pol oscillator driven by Gaussian colored noise.

In this paper, we explore the effects of additive and multiplicative Gaussian colored noises on a bistable Duffing–Van der Pol oscillator. Furthermore, one can find the relation of stochastic bifurcation and noise correlation time on the dynamical properties. Based on the stochastic averaging method to separate fast and slow variables of the oscillator, the bifurcation analysis will be presented, taking the system parameters and statistical characteristics of noise (e.g., noise intensity and noise correlation time) as bifurcation parameters. Two types of qualitative changes are observed, and bifurcation diagrams of the system in different parameter planes are presented. We find that the effects of multiplicative noise and that of additive noise are quite different (or not directly related).

This paper is organized as follows. In Sec. II, the stochastic averaging method theoretically is carried out to obtain the stationary probability density function of amplitude for the noisy Duffing–Van der Pol oscillator. Then, the stochastic *P* bifurcations are discussed in Sec. III. Here, we analyze the influence of the noise correlation time and noise intensity on stochastic *P* bifurcations in two cases of additive noise and

*hsux3@nwpu.edu.cn

 

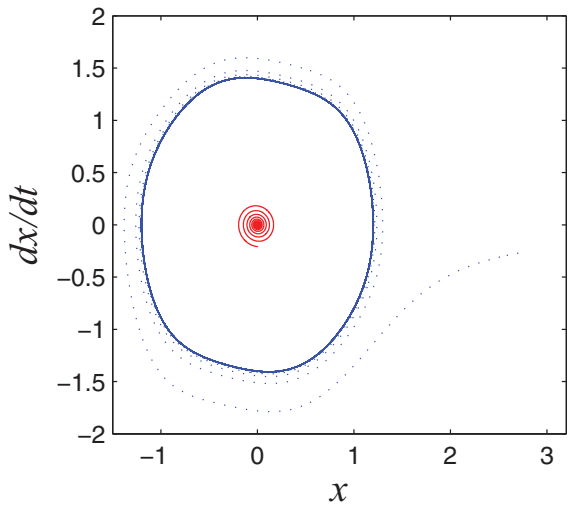


FIG. 1. (Color online) Two attractors of system Eq. (1) for $D = 0$ when $\varepsilon = -0.11$ and $\beta_1 = \beta_2 = 1.0$.

multiplicative noises. Finally, Sec. IV is devoted to concluding remarks and discussions.

## II. STATIONARY PROBABILITY DISTRIBUTION OF A BISTABLE OSCILLATOR WITH GAUSSIAN COLORED NOISE

In this section, we consider a bistable Duffing–Van der Pol oscillator with colored Gaussian noise,

$$\ddot{x} - (\varepsilon + \beta_1 x^2 - \beta_2 x^4)\dot{x} + x + \beta_0 x^3 = \eta(t) + x\xi(t), \quad \beta_i \geqslant 0, \tag{1}$$

where $\varepsilon$, $\beta_0$, $\beta_1$, and $\beta_2$ are real parameters ($\beta_0$is a small parameter), while $\eta(t)$ and $\xi(t)$ are Gaussian colored noises with zero mean and correlation,

$$\begin{aligned} \langle \eta(t)\eta(s)\rangle &= \frac{D_1}{\tau_1}\exp\left[-\frac{|t-s|}{\tau_1}\right], \\ \langle \xi(t)\xi(s)\rangle &= \frac{D_2}{\tau_2}\exp\left[-\frac{|t-s|}{\tau_2}\right], \\ \langle \eta(t)\xi(s)\rangle &= 0. \end{aligned} \tag{2}$$

Here $\tau_1, \tau_2$ and $D_1, D_2$ denote the correlation time and intensity of the colored noises $\eta(t)$ and$\xi(t)$, respectively.

In the deterministic case ($D_1 = D_2 = 0$), when $-\frac{\beta_1}{8\beta_2} < \varepsilon < 0$, the system in Eq. (1) is characterized with a bistable behavior: Two attractors are in the phase plane: a stable focus at the origin and a stable limit cycle, as Fig. 1 shows. Thus, the bistability region is restricted to a saddle-node bifurcation of cycles at $\varepsilon = -\beta_1/8\beta_2$ and a subcritical Andronov-Hopf bifurcation at $\varepsilon = 0$. Furthermore, the parameter $\beta_0$ defines the anisochronicity of oscillations: For $\beta_0 = 0$, the nonisochronicity of the system in Eq. (1) is quite small.

When $D_1 \neq 0$ and/or $D_2 \neq 0$, we assume that the noise intensity is small and introduce a change of variables,

$$x(t) = a\cos\theta, \quad x(t) = -a\sin\theta, \quad \theta = t + \varphi. \tag{3}$$

Substituting Eq. (3) into Eq. (1), we can obtain

$$\begin{cases} \dot{a} = a\sin^2\theta(\varepsilon + \beta_1 a^2\cos^2\theta - \beta_2 a^4\cos^4\theta) \\ \quad\quad +\beta_0 a^3\cos^3\theta\sin\theta - \sin\theta\eta(t) - a\sin\theta\cos\theta\xi(t) \\ \dot{\varphi} = \sin\theta\cos\theta(\varepsilon + \beta_1 a^2\cos^2\theta - \beta_2 a^4\cos^4\theta) \\ \quad\quad +\beta_0 a^2\cos^4\theta - \frac{\cos\theta}{a}\eta(t) - \cos^2\theta\xi(t) \end{cases} \tag{4}$$

By applying the stochastic averaging method [22,23], we can obtain the following pair of stochastic equations for amplitude $a(t)$ and phase $\varphi(t)$:

$$\begin{cases} da = \left[\frac{\varepsilon a}{2} + \frac{\beta_1 a^3}{8} - \frac{\beta_2 a^5}{16} + \frac{3D_2 a}{8\left(1+4\tau_2^2\right)} + \frac{D_1}{2a\left(1+\tau_1^2\right)}\right]dt \\ \quad\quad +\sqrt{\frac{D_1}{1+\tau_1^2} + \frac{D_2 a^2}{4\left(1+4\tau_2^2\right)}}\,dW_1(t), \\ d\varphi = \left(\frac{3\beta_0 a^2}{8} - \frac{D_2\tau_2}{2\left(1+4\tau_2^2\right)}\right)dt \\ \quad\quad +\sqrt{\frac{D_1}{\left(1+\tau_1^2\right)a^2} + \frac{2D_2\tau_2^2}{1+4\tau_2^2} + \frac{3D_2}{4\left(1+4\tau_2^2\right)}}\,dW_2(t), \end{cases} \tag{5}$$

where $W_1(t)$ and $W_2(t)$ represent independent normalized Wiener processes. Clearly, $da$ does not depend on $\varphi$, thus, we can develop a probability density for $a$, rather than a joint density for $a$ and $\varphi$.

The probability density function $p(a,t\,|a_0,t_0)$ for amplitude is governed by the Fokker-Planck-Kolmogorov equation,

$$\begin{aligned} \frac{\partial p}{\partial t} = &\left[\left(\frac{\varepsilon a}{2} + \frac{\beta_1 a^3}{8} - \frac{\beta_2 a^5}{16} + \frac{3D_2 a}{8\left(1+4\tau_2^2\right)} + \frac{D_1}{2a\left(1+\tau_1^2\right)}\right)p\right] \\ &+\frac{1}{2}\left(\frac{D_1}{\left(1+\tau_1^2\right)} + \frac{D_2 a^2}{4\left(1+4\tau_2^2\right)}\right)\frac{\partial^2 p}{\partial a^2}. \end{aligned} \tag{6}$$

By letting $\frac{\partial P(a,t)}{\partial t} = 0$, according to Zhu [22], the stationary solution of Eq. (6) is

$$p(a) = \frac{N}{B(a)}\exp\left[2\int\frac{A(a)}{B(a)}da\right], \tag{7}$$

where

$$\begin{aligned} A(a) &= \left(\frac{\varepsilon a}{2} + \frac{\beta_1 a^3}{8} - \frac{\beta_2 a^5}{16} + \frac{3D_2 a}{8(1+4\tau_2^2)} + \frac{D_1}{2a(1+\tau_1^2)}\right), \\ B(a) &= \left(\frac{D_1}{(1+\tau_1^2)} + \frac{D_2 a^2}{4(1+4\tau_2^2)}\right), \end{aligned} \tag{8}$$

where $N$ is a normalization constant.

## III. STOCHASTIC BIFURCATIONS

This section is devoted to discussing stochastic bifurcations through qualitative changes of the stationary probability density $p(a)$. The exact probability densities are presented in the case of additive noise and the case of combined multiplicative noise and additive noise, respectively. The number and the extrema of the stationary densities have been carefully examined.

### A. The case of additive colored noise

We first consider system (1) with only additive colored noise with $D_2 = 0, D_1 \neq 0$. By Eqs. (7) and (8), we get

$$p(a) = N\left(1+\tau_1^2\right) a \exp\left[\frac{1+\tau_1^2}{48D_1}(24\varepsilon a^2 + 3\beta_1 a^4 - \beta_2 a^6)\right], \tag{9}$$

where $N$ is a normalization constant.

In the limit $\tau_1 \to 0$, the colored noise $\eta(t)$ tends to a white noise, and this case was discussed in Ref. [13]. From Eq. (9), we find that the shape of amplitude in Eq. (5) does not depend on phase $\varphi$ and system parameter $\beta_0$.

Moreover, by letting $\frac{\partial p(a)}{\partial a} = 0$, the extrema of the distribution Eq. (9) become the roots of

$$a_m^6 - 2\frac{\beta_1}{\beta_2}a_m^4 - \frac{8\varepsilon}{\beta_2}a_m^2 - \frac{8D_1}{\beta_2\left(1+\tau_1^2\right)} = 0, \tag{10}$$

where $a_m$ is the amplitude corresponding to the extremum of distribution Eq. (9) and $m$ is the index number of the extremum. The number of real roots of Eq. (10) is either 1 or 3 for different parameters, which represents the unimodal distribution and the bimodal distribution of the amplitude, respectively. This effect means that a type of stochastic bifurcation will take place. It is necessary to note that the transitions between the unimodal and the bimodal stationary probability densities are also referred to as the noise-induced transitions, and stochastic bifurcation discussed here is closely connected to the noise-induced transition [24].

In the parameter plane of $D_1$ and $\tau_1$, Fig. 2(a) displays the bifurcation graph of system (5) from the analysis of Eq. (10) with parameters $\varepsilon = -0.14$ and $\beta_1 = \beta_2 = 1.0$. The stationary amplitude distribution is bimodal in the tinted region and unimodal in the colorless region. The lines $l_1$ and $l_2$ represent the appearance and disappearance of one of the maxima of $p(a)$ that bounds the region corresponding to stochastic $P$ bifurcation. By increasing $\tau_1$, the bimodality region will shift to larger values of $D_1$ and will become wider. The numerical solutions of the oscillator Eq. (1) could be obtained by an order-2 stochastic Runge-Kutta algorithm [25] with initial conditions $t_0 = 0, x(0) = 0.2$, and $\dot{x}(0) = 0.1$ by taking the parameter $\beta_0 = 0.1$ and the time step $\Delta t = 0.01$ in numerical calculations. As $a(t) = \sqrt{x(t)^2 + \dot{x}(t)^2}$, then the stationary probability density function $p(a)$ can be obtained by the Monte Carlo simulation method with the simulation data length $N = 10^7$. With parameters $\tau_1 = 0.5, \varepsilon = -0.14$, and $\beta_1 = \beta_2 = 1.0$, we demonstrate the figure of stationary probability density for amplitude versus different noise intensity $D_1$ in Fig. 2(b). One can observe that the amplitude distribution has only one maximum situated in the vicinity of zero when the noise intensity is small. As $D_1 \approx 0.0182$ [see point $A$ in Fig. 2(a)], a transition from a unimodal to a bimodal distribution occurs, and for $D_1 \approx 0.03$ [point $B$ in Fig. 2(a)], the second stochastic bifurcation will appear. The amplitude distribution becomes unimodal again, but its maximum is shifted toward larger amplitude values, as curve 3 in Fig. 2(b) depicts.

Additionally, by fixing $D_1 = 0.05$ and $\beta_1 = \beta_2 = 1.0$, we consider the influence of noise correlation time on the stochastic $P$ bifurcation. The bifurcation diagram of system (5) in the parameter plane $(\varepsilon, \tau_1)$ is given in Fig. 3(a). According to the previous similar discussions concerning Fig. 2(a), the stationary amplitude distribution is bimodal in the tinted region and unimodal in the gap region. Lines $l_3$ and $l_4$ are boundaries of the tinted region, which mean stochastic $P$ bifurcations. By decreasing the value of $\varepsilon$, the bimodal region shifts to smaller values of $\tau_1$ and becomes narrow. If $\varepsilon$ is decreased further (e.g., for $\varepsilon < \varepsilon_1 \approx -0.155$), then the bimodality region does not exist anymore, and the $P$ bifurcation cannot be observed for any correlation time. For the fixed noise intensity $D_1 = 0.05$ and parameter $\varepsilon = -0.11$, Fig. 3(b) shows the stationary probability density of amplitude with different values of correlation time $\tau_1$. In this case, there are two attractors in the deterministic system, see Fig. 1. For the short correlation time

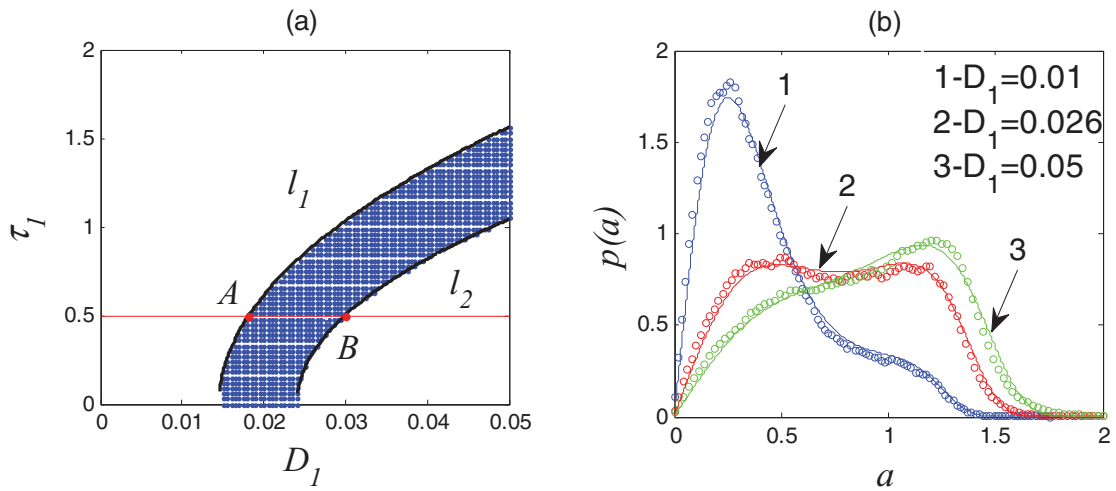


FIG. 2. (Color online) Stochastic $P$ bifurcations in the Duffing–Van der Pol oscillator [Eqs. (1) and (5)]. (a) Bifurcation diagram of system (5) in the parameter plane $(D_1, \tau_1)$ for $\varepsilon = -0.14$ and $\beta_1 = \beta_2 = 1.0$. Points $A$ and $B$ are intersection points of the horizontal dashed line $\tau_1 = 0.5$ and $l_1$,$l_2$, respectively. (b) Stationary probability density of amplitude for $\tau_1 = 0.5, \varepsilon = -0.14$, and $\beta_1 = \beta_2 = 1.0$ and different values of noise intensity. The solid lines denote the algebraic calculations using Eq. (9), whereas, the normalization constant $N$ is defined numerically. The circles represent the numerical solutions for the oscillator Eq. (1).

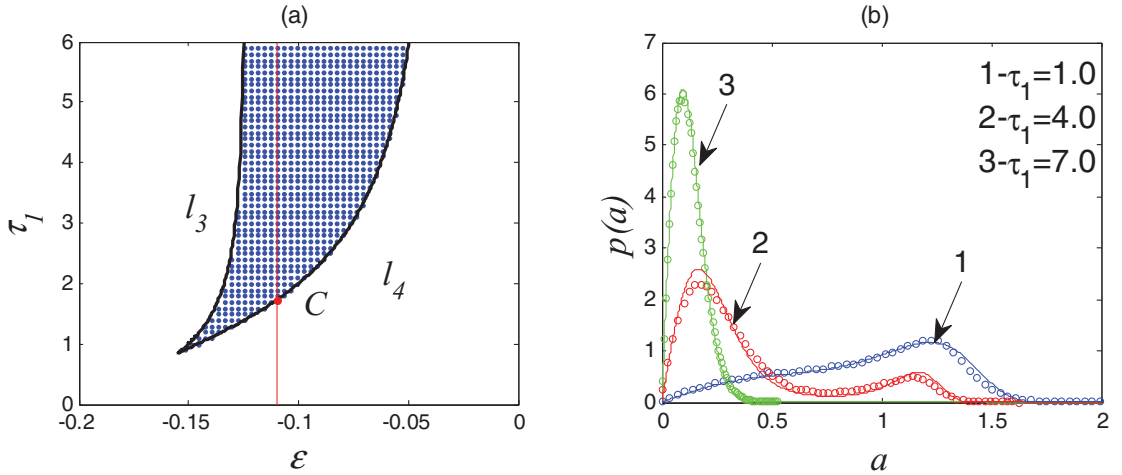


FIG. 3. (Color online) Stochastic $P$ bifurcations in the Duffing–Van der Pol oscillator [Eqs. (1) and (5)] for $D_1 = 0.05$ and $\beta_1 = \beta_2 = 1.0$. (a) Bifurcation diagram of system (5) in the parameter plane $(\varepsilon, \tau_1)$. Point $C$ is the intersection point of the vertical dashed line $\varepsilon = -0.11$ and $l_4$. (b) Stationary probability density of amplitude for $\varepsilon = -0.11 and D_1 = 0.05$ and different values of correlation time. The solid lines and circles have the same meaning as in Fig. 2(b).

[below point $C$ in Fig. 3(a)], the amplitude distribution has only one peak, as curve 1 in Fig. 3(b) shows, and for $\tau_c \approx 1.72$, a transition from a unimodal to a bimodal distribution occurs, which can be found in curve 2 of Fig. 3(b). Additionally, it should be worth noticing that the stationary probability density $p(a)$ remains bimodal as $\tau_1$ increases ($\tau_1 > \tau_c$). However, the value of the peak, which corresponds to a larger amplitude, becomes very small if the correlation time is large (e.g., for $\tau_1 > 6.0$), as curve 3 in Fig. 3(b) shows. The phase trajectory visits the regions close to the origin more and more frequently, and the nonlinearity of the system becomes weak.

### B. The case of multiplicative and additive colored noises

With $D_1 = 0$ and $D_2 \neq 0$, the random noisy oscillator will be reduced to a Duffing–Van der Pol system excited by the multiplicative noise, and the stationary probability density function due to Eq. (7) for amplitude can be obtained as

$$p(a) = N a^{1+\varepsilon/L} \exp\left(\frac{4\beta_1 a^2 - \beta_2 a^4}{32L}\right), \tag{11}$$

where $L = \frac{D_2}{4(1+4\tau_2^2)}$ and $N$ is a normalization constant.

By letting $p(a) = 0$, the extrema of the distribution Eq. (11) are the roots of

$$a_m^4 - \frac{2\beta_1}{\beta_2} a_m^2 - \frac{8(L+\varepsilon)}{\beta_2} = 0. \tag{12}$$

The real positive root of Eq. (12) is $\sqrt{\frac{\beta_1}{\beta_2} + \sqrt{\frac{\beta_1^2}{\beta_2^2} + \frac{8(L+\varepsilon)}{\beta_2}}}$ for $\varepsilon > -L$, and then the probability density function in Eq. (11) has a maximum [curve 2 in Fig. 4(a)]. With $\varepsilon \leqslant -L$,

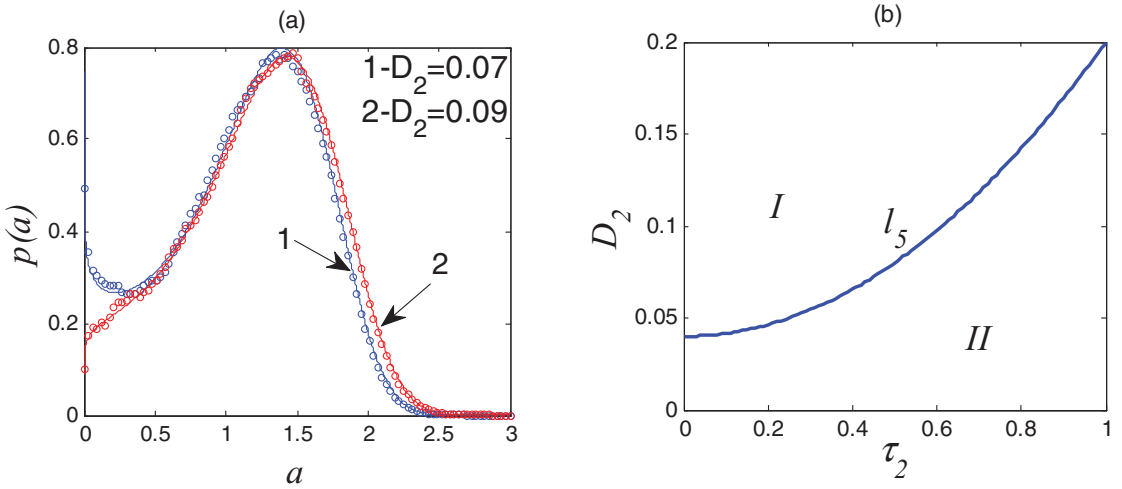


FIG. 4. (Color online) Stochastic $P$ bifurcations in the Duffing–Van der Pol oscillator excited by multiplicative noise for$\varepsilon = -0.01$. (a) Stationary probability density for $\tau_2 = 0.5$ and $\beta_1 = \beta_2 = 0.1$ and different $D_2$'s. (b) Bifurcation diagram of system (5) in the parameter plane $(\tau_2, D_2)$. Line $l_5$ is the boundary of regions $I$ and $II$.

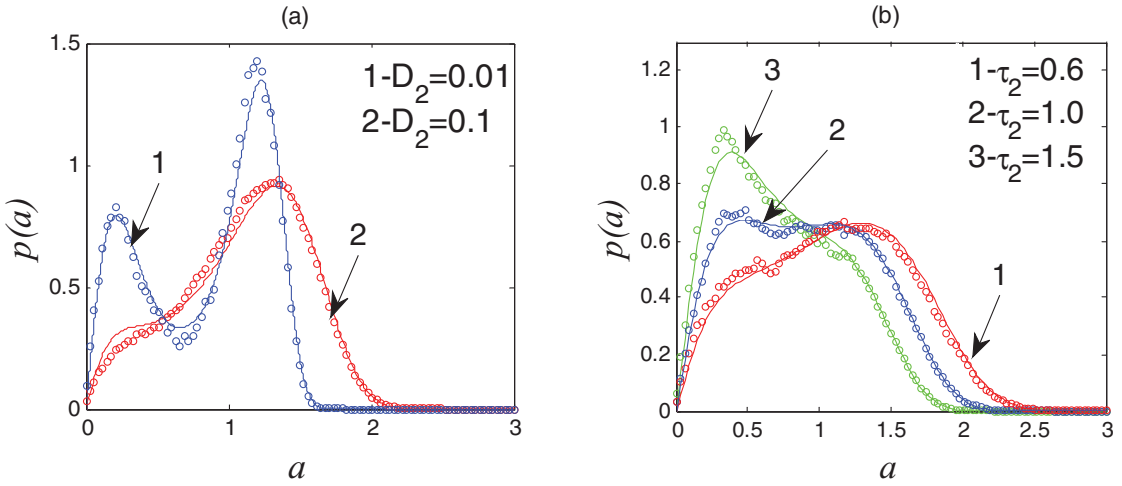


FIG. 5. (Color online) Stationary probability density for $\varepsilon = -0.01$ and appropriate parameters. The solid lines denote the algebraic calculations using Eq. (13), whereas, the normalization constant $N$ is defined numerically. The circles represent the numerical solutions for the oscillator Eq. (1) by the same algorithm as in Fig. 1(b). (a) $\beta_1 = \beta_2 = 0.1, D_1 = 0.01, \tau_1 = 5.0$, and $\tau_2 = 1.0$, different values of $D_2$; (b) $\beta_1 = \beta_2 = 0.05, D_1 = 0.005, D_2 = 0.06$, and $\tau_1 = 2.0$, different values of $\tau_2$.

there are two real positive roots of Eq. (12), whose shape is similar to a crater, and the probability density $p(a)$ has a minimum and a maximum, respectively, as curve 1 in Fig. 4(a) shows. Thus, a transition from a craterlike density to a unimodal density is observed, which can be defined as a type of $P$ bifurcation, and this is completely different from the case of additive noise. It should be noticed that Eq. (11) is a singular integral, which is singular at $a = 0$ for $\varepsilon < -L$. However, on the basis of the convergence criterion of the singular integral, we can find that Eq. (11) is integrable in the condition of $\varepsilon > -2L$. For $\varepsilon = -0.01$, the bifurcation diagram of system (5) in the parameter plane $(\tau_2, D_2)$ is given in Fig. 4(b), where, in region $II$, the stationary amplitude is a craterlike distribution, and region $I$ represents the unimodal distribution. Line $l_5$ denoted the boundary of regions $I$ and $II$ corresponding to stochastic $P$ bifurcations.

If $D_1 \neq 0$ *and* $D_2 \neq 0$, system (1) will be driven by a combination of multiplicative and additive colored noises.

According to Eqs. (7) and (8), we have

$$p(a) = Na\left(K + La^2\right)^Q \times \exp[(4\beta_1 La^2 + 2\beta_2 Ka^2 - \beta_2 La^4)/32L^2], \tag{13}$$

where $K = \frac{D_1}{1+\tau_1^2}, L = \frac{D_2}{4(1+4\tau_2^2)}$, and $Q = (8\varepsilon L^2 - 2\beta_1 KL - \beta_2 K^2)/16L^3$.

Similarly, by letting $p(\dot{a}) = 0$, the extrema of distribution Eq. (13) are the roots of the equation,

$$a_m^6 - ha_m^4 - ma_m^2 - n = 0, \tag{14}$$

with $h = \frac{2\beta_1}{\beta_2}$, $m = \frac{16QL^3 + 8L^3 + 2\beta_1 KL + \beta_2 K^2}{\beta_2 L^2}$, and $n = \frac{8K}{\beta_2}$.

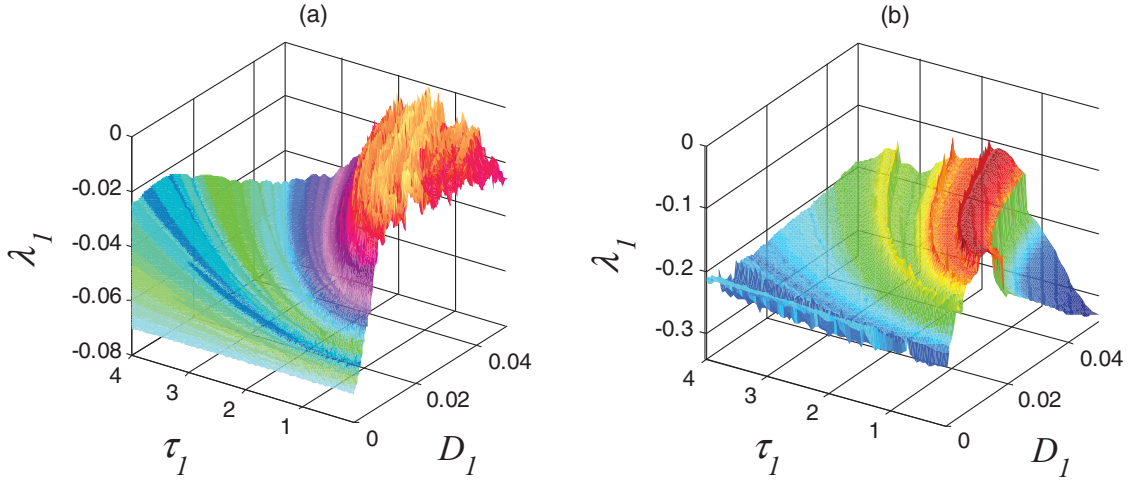


FIG. 6. (Color online) The largest Lyapunov exponent $\lambda_1$ in the $(D_1, \tau_1)$ plane of the additive noise case for $\varepsilon = -0.14$ and $\beta_1 = \beta_2 = 1.0$, refer to Fig. 2(a). (a) The largest Lyapunov exponent of the original system Eq. (1). (b) The largest Lyapunov exponent of the averaged system Eq. (5).

By taking $\varepsilon = -0.01, \beta_1 = \beta_2 = 0.1, D_1 = 0.01, D_2 = 0.01$, $\tau_1 = 5.0$, and $\tau_2 = 1.0$, the roots of Eq. (14) are 0.215, 0.67, and 1.23, which represent the corresponding amplitude of maximum, minimum, and maximum of the stationary probability density in Eq. (13), respectively, as curve 1 in Fig. 5(a) shows. Curve 2 in Fig. 5(a) is unimodal for $D_2 = 0.1$, and other parameters are the same as curve 1. Thus, there will be a stochastic $P$ bifurcation when the multiplicative noise intensity $D_2$ increases from 0.01 to 0.1. To fix $\varepsilon = -0.01, \beta_1 = \beta_2 = 0.05, D_1 = 0.005, D_2 = 0.06, and \tau_1 = 2.0$, the stationary amplitude distribution in Eq. (13) with different $\tau_2$'s is shown in Fig. 5(b), where $p(a)$ is unimodal for $\tau_2 = 0.5$; see curve 1 in Fig. 5(b). As $\tau_2$ increases to 1.0, the stationary probability density function becomes bimodal; it changes to unimodal if $\tau_2 = 1.5$, as shown in Fig. 5(b), curves 2 and 3. In other words, two stochastic $P$ bifurcations take place when multiplicative noise correlation time $\tau_2$ increases. Therefore, the type of stochastic $P$ bifurcations induced by multiplicative noise will vary when the system is excited by additive noise as well. For instance, a transition between craterlike density and unimodal density will be changed to a transition between unimodal density and bimodal density. Moreover, according to the number of the real roots of Eq. (14), bifurcation diagrams in different planes can be obtained, but we omit them here.

It is worthy to note that the average model Eq. (5) does not completely reflect the properties of the original system for large values of noise intensity and correlation time. However, it can be found that the analytical solutions agree well with the numerical results from the figures we presented in this paper. Additionally, the bifurcation diagrams are related not only to the average model, but also to the original system and do not depend on the parameter of anisochronicity $\beta_0 \geqslant 0$. Here, we point out that one can find appropriate parameter ranges for $\varepsilon$, $\beta_1$, $\beta_2$, $D_1$, $D_2$, $\tau_1$, and $\tau_2$ from expressions of the stationary probability density $p(a)$ [see Eqs. (9), (11), and (13)].

Now, we apply the numerical algorithm in Refs. [26,27] to numerically calculate the largest Lyapunov exponent of the initial system Eq. (1) and the average system Eq. (5) for the additive noise case with $\varepsilon = -0.14 and \beta_1 = \beta_2 =$ 1.0, which are shown in Fig. 6. The figures show the top Lyapunov exponent $\lambda_1$ remains negative for any $(D_1, \tau_1) \in (0 \sim 0.05, 0 \sim 4.0)$, so the stochastic bifurcation cannot be found based on the sudden change of sign of the largest Lyapunov exponent. Additionally, $P$ bifurcation is nearly independent of $\beta_0$, while for $D$ bifurcation, this parameter is crucial, i.e., $P$ bifurcation is not necessarily accompanied by $D$ bifurcation.

## IV. CONCLUDING REMARKS

In this paper, we have presented results about stochastic bifurcations in a self-sustained bistable Duffing–Van der Pol oscillator with additive and/or colored noise. By applying a method of stochastic averaging based on a perturbation technique, we obtained the stationary probability density function of amplitude for the noisy oscillator. Two types of qualitative change were found, namely, a transition from unimodal density to bimodal density and a transition from craterlike density to unimodal density. The stochastic bifurcations based on the qualitative change of stationary measures were observed by discussing the extrema of the distribution. Bifurcation diagrams of the system in various parameter planes were obtained, and from which we pointed out that not only system parameters and noise intensity can be treated as the bifurcation parameter, but also change of noise correlation time could induce stochastic bifurcations. Besides, the investigations showed that the effects of multiplicative noise were different from that of additive noise. In addition, the $D$ bifurcation via the change of the largest Lyapunov exponent appeared not to agree well with the results of $P$ bifurcation, and we remarked that there was no direct connection between these two stochastic bifurcations.

## ACKNOWLEDGMENTS

This work was supported by the NSF of China (Grants No. 10972181, No. 11002001, and No. 10872165), the Northwestern Polytechnical University Foundation for Fundamental Research, and the Aoxiang Star Plan of NPU. The authors thank the referees for their very valuable suggestions.

[1] O. V. Ushakov, H. J. Wünsche, F. Henneberger, I. A. Khovanov, L. Schimansky-Geier, and M. A. Zaks, Phys. Rev. Lett. **95**, 123903 (2005).
[2] R. Mankin, T. Laas, A. Sauga, A. Ainsaar, and E. Reiter, Phys. Rev. E **74**, 021101 (2006).
[3] Y. K. Lin and G. Q. Cai, *Probabilistic Structure Dynamic: Advanced Theory and Applications* (McGraw-Hill, New York, 1995).
[4] N. Sri Namachchivaya and W. M. Tien, J. Fluids Struct. **3**, 609 (1989).
[5] N. Sri Namachchivaya, Appl. Math. Comput. **38**, 101 (1990) .
[6] L. Billings, I. Schwartz, D. Morgan, E. Bollt, R. Meucci, and E. Allaria, Phys. Rev. E **70**, 026220 (2004).
[7] W. Xu, Q. He, T. Fang, and H. Rong, Int. J. Non-Linear Mech. **39**, 1473 (2004).
[8] Q. He, W. Xu, H. Rong, and T. Fang, Physica A **338**, 319 (2004).
[9] C. Chiarella, X. Zhong He, D. Wang, and M. Zheng, Physica A **387**, 3837 (2008).
[10] S. Wieczorek, Phys. Rev. E **79**, 036209 (2009).
[11] H. Nakao, J. N. Teramae, D. S. Goldobin, and Y. Kuramoto, Chaos **20**, 033126 (2010).
[12] D. S. Goldobin and A. Pikovsky, Phys. Rev. E **71**, 045201(R) (2005).
[13] A. Zakharova, T. Vadivasova, V. Anishchenko, A. Koseska, and J. Kurths, Phys. Rev. E **81**, 011106 (2010).
[14] H. Hasegawa, Physica D **237**, 137 (2008).
[15] L. Arnold, *Random Dynamical Systems* (Springer, New York, 1998).
[16] D. S. Goldobin, J.-n. Teramae, H. Nakao, and G. B. Ermentrout, Phys. Rev. Lett. **105**, 154101 (2010).

[17] D. S. Goldobin and A. Pikovsky, Phys. Rev. E **73**, 061906 (2006).
[18] A. Drozd-Rzoska, S. J. Rzoska, and J. Zioło, Phys. Rev. E **61**, 5349 (2000).
[19] C. R. Doering and J. C. Gadoua, Phys. Rev. Lett. **69**, 2318 (1992).
[20] P. Holmes and D. Rand, Int. J. Non-Linear Mech. **15**, 449 (1980).
[21] J. Guckenheimer and P. Holmes, *Nonlinear Oscillation Dynamical Systems and Bifurcation of Vector Fields* (Springer, Berlin, 1983).
[22] W. Zhu, Appl. Mech. Rev. **49**, s72 (1996).
[23] J. Roberts and P. Spanos, Int. J. Non-Linear Mech. **21**, 111 (1986).
[24] W. Horsthemke and R. Lefever, *Noise-Induced Transitions: Theory and Applications in Physics, Chemistry, and Biology*, 2nd ed. (Springer-Verlag, Berlin/Heidelberg, 2007).
[25] R. L. Honeycutt, Phys. Rev. A **45**, 604 (1992).
[26] G. Benettin, L. Galgani, and A. Giorgilli, Meccanica **15**, 21 (1980).
[27] L. Arnold, P. Imkeller, and N. Sri Namachchivaya, J. Sound Vib. **269**, 1003 (2004).